

Preparation and Properties of Wet-Spun Microcomposite Filaments from Cellulose Nanocrystals and Alginate Using a Microfluidic Device

Ji-Soo Park,^{a,e} Chan-Woo Park,^b Song-Yi Han,^b Eun-Ah Lee,^{a,b} Azelia Wulan Cindradewi,^{a,b} Jeong-Ki Kim,^{a,b} Gu-Joong Kwon,^{b,c} Young-Ho Seo,^d Won-Jae Youe,^e Jaegyong Gwon,^e and Seung-Hwan Lee^{a,b,*}

Cellulose nanocrystals (CNCs) were wet-spun in a coagulation bath for the fabrication of microfilaments, and the effect of sodium alginate (AL) addition on the wet-spinnability and properties of the microcomposite filament was investigated. The CNC suspension exhibited excellent wet-spinnability in calcium chloride (CaCl₂) solution, and the addition of AL in CNC suspension resulted in the enhancement of the wet-spinnability of CNCs. As the AL content increased from 3% to 10%, the average diameter of the microcomposite filament decreased, and its tensile properties deteriorated. The increased spinning rate caused an increase in the orientation index of CNCs, resulting in an improvement in the tensile properties of the microcomposite filament.

Keywords: Cellulose nanocrystal; Alginate; Wet-spinning; Microcomposite filament

Contact information: a: Department of Forest Biomaterials Engineering, College of Forest and Environmental Sciences, Kangwon National University, Chuncheon 24341, Republic of Korea; b: Institute of Forest Science, Kangwon National University, Chuncheon 24341, Republic of Korea; c: Kangwon Institute of Inclusion Technology, Kangwon National University, Chuncheon 24341, Republic of Korea; d: Department of Advanced Mechanical Engineering, Kangwon National University, Chuncheon 24341, Republic of Korea; e: National Institute of Forest Science, Seoul 02455, Republic of Korea; * Corresponding author: lshyhk@kangwon.ac.kr

INTRODUCTION

Nanocellulose is a cellulosic nanomaterial with nanoscale dimensions (Lee *et al.* 2019). Nanocellulose has various excellent properties, such as biodegradability, sustainability, low density, low swelling-shrinkage, high strength, and large specific surface area (Abitbol *et al.* 2016; Lee *et al.* 2019). Therefore, nanocellulose is considered a promising material for the development of functional materials and high-strength composites. It can be applied to films, bioplastics, adsorbents, drug delivery systems, biomedical materials, *etc.* (Sen *et al.* 2015; Ávila *et al.* 2016; Hubbe *et al.* 2017; Tan *et al.* 2019; Köse *et al.* 2020). In the textile industries, the application of nanocellulose is expected to be extremely beneficial (Iwamoto *et al.* 2011; Lundahl *et al.* 2016a,b; Kafy *et al.* 2017; Park *et al.* 2020).

Conventionally, regenerated cellulosic fibers have been used as long filaments in the textile field and can be produced by dissolving cellulose in solvents, such as N-methylmorpholine N-oxide, NaOH solution, and cuprammonium solution (Sayed *et al.* 2019). However, these manufacturing processes use harmful chemicals and require large amounts of energy to recover the solvents (Lennartsson *et al.* 2011; Sayyed *et al.* 2019). To produce filaments from natural cellulose without dissolving and regenerating cellulose,

spun yarn is fabricated by twisting several short cellulosic fibers with initially short lengths of 10 to 70 mm, although diameters in microns have been used. However, yarn normally has a lower strength than the regenerated cellulosic filament. Recently, the wet-spinning process of nanocellulose suspensions has been promising for the development of high-strength filaments. Nanocellulose is not soluble in water and can be highly dispersed with high viscosity. This characteristic is beneficial for wet-spinning for filament production (Iwamoto *et al.* 2011; Syverud *et al.* 2015; Kafy *et al.* 2017). The spinnability and characteristics of wet-spun filaments can be adjusted depending on the type of nanocellulose, spinner needle size, spinning rate, and collecting solvent. During the drying process of the wet-spun nanocellulose filament, strong hydrogen bonding occurs between the nanofibrils, resulting in an extremely high strength and elastic modulus (Lundahl *et al.* 2016a,b). The tensile strength and elastic modulus of the wet-spun nanocellulose filaments are 100 to 400 MPa and 7 to 10 GPa, respectively (Iwamoto *et al.* 2011; Lundahl *et al.* 2016a,b; Kafy *et al.* 2017). These enhanced mechanical properties are advantageous for the application of nanocellulose filaments in the textile industry. Moreover, the properties, functionality, and applicability of the wet-spun filaments from nanocellulose can be improved by blending hydrophilic biopolymers, such as sodium alginate (AL), owing to the strong hydrogen bonding between the hydroxyl group of nanocellulose and carboxyl group of AL (Zhang and Luo 2011; Liu *et al.* 2019). These wet-spun nanocellulose-derived composite filaments with AL have strong potential for application in fiber-reinforced composites, hygiene products, and biomedical products, among others (Khalil *et al.* 2015; Lundahl *et al.* 2016a,b). Normally, microneedles of 300 to 1000 μm are used for wet-spinning nanocellulose. The filament can be designed and controlled at micro and nano sizes through microneedles used in microfluidic spinning (Nechporchuk and Köhnke 2018).

The microfluidic system manipulates fluids in channels with dimensions of tens of micrometers (Whitesides 2006). This system has gained interest in recent years because of its significant potential for producing micro- and nano-scale structures with diverse shapes, such as particles, filaments, and tubes (Jun *et al.* 2014). In particular, microfluidic wet-spinning method has attracted attention for the fabrication of microfilaments (Nechporchuk and Köhnke 2018; Gursoy *et al.* 2020) owing to its high suitability for adjusting the diameter at a microscale and for the formation of co-axial filaments. The resulting microfilaments can be applied in many fields, such as chemistry, biology, medicine, and physical sciences (Shang *et al.* 2019). Microfluidic channel devices can be manufactured using metal, glass, and polydimethylsiloxane (PDMS) (Plečis and Chen 2007). In particular, PDMS has been widely used for microfluidic channels owing to its low cost, simple preparation, excellent mechanical properties, biocompatibility, and resistance to oxidation and ultraviolet rays (Xia and Whitesides 1998).

In recent years, various microcomposite filaments have been prepared using AL, chitosan, and collagen (Lee *et al.* 2011; Bonhomme *et al.* 2012; Haynl *et al.* 2016) through the microfluidic channels. Nanocellulose can also be fabricated into microcomposite filaments through a microfluidic system (Nechporchuk and Köhnke 2018). In particular, cellulose nanocrystal (CNC) is highly suitable for microfluidic wet-spinning because it has a small diameter of 4 to 6 nm and short length in the range of 100 to 500 nm (Habibi *et al.* 2010; Cheng *et al.* 2017). Therefore, it is expected that CNC can be well-oriented along the axial of microcomposite filaments in the microfluidic channel by shearing force generated by microfluidic wet-spinning. The wet-spun microcomposite filament from CNC has high potential for application in hygiene and biomedical products, including wound

dressing, wound healing, and hemostasis (Nechyporchuk and Köhnke 2018). However, most of the previous studies have been focused on using CNC as reinforcement, while the preparation of CNC filaments has been less explored. CNCs with sulfate groups have extremely high dispersibility in polar solvents (Xu *et al.* 2013) and good affinity with hydrophilic biopolymers, such as AL, which can act as a binder between CNCs.

In this study, microcomposite filaments were prepared by microfluidic wet-spinning of a CNC/AL suspension using PDMS microfluidic channel. The effects of the AL content, spinning suspension concentration, and spinning rate on the wet-spinnability and properties of the microcomposite filament were investigated. To the best of author's knowledge, this is the first report on preparation of CNC filament where AL is used as filler.

EXPERIMENTAL

Materials

CNC with a diameter of 4 to 7 nm was supplied by Cellulose Lab Co., Ltd. (QC, Canada). AL, calcium chloride (CaCl_2), isopropyl alcohol, 1,4-dioxane, and sodium polyacrylate were purchased from Daejung Chemical & Metals Co., Ltd. (Siheung, Republic of Korea). To form the microfluidic channel, PDMS (Sylgard-184) was purchased from Dow Corning Co., Ltd. (Barry, UK) and polyethylenimine (PEI) for the coating of CNC on a mica surface was purchased from Wako Pure Chemical Industries, Ltd. (Osaka, Japan). All the chemicals were used without further purification.

Preparation of Microfluidic Channel

Through a photolithography process, a microfluidic channel mold with a size of $0.2 \times 0.1 \times 70$ mm (width \times height \times length) was manufactured using a SU-8 2100 (MicroChem, Inc., MA, USA) photoresist. PDMS was used to replicate the microfluidic channel from the microfluidic channel mold and then bonded to the bottom plate to complete the microfluidic channel by plasma treatment.

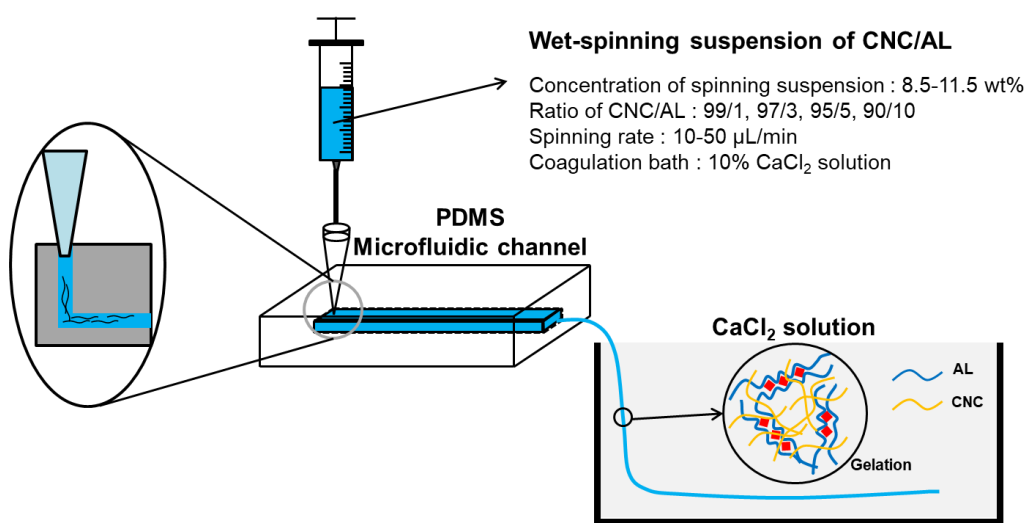


Fig. 1. Schematic of CNC/AL spinning suspension loading procedure through a PDMS microfluidic channel

Preparation of Wet-spun Microcomposite Filament

AL (17.5 g) was dissolved in distilled water (482.5 g) at 60 °C for 12 h under constant stirring at 200 rpm to form a 3.5 wt% concentration of AL solution. The prepared AL solution was mixed with CNC suspension at a ratio of 99/1, 97/3, 95/5, and 90/10 (CNC/AL). After installing the syringe in the microfluidic channel, spinning suspensions of CNC/AL at concentrations of 8.5 and 11.5 wt% were wet-spun in a coagulation bath of 10% CaCl₂ solution. The spinning rates were set to 10 and 50 μL/min. The obtained wet-spun microcomposite filaments were air-dried for 24 h and then oven-dried at 100 °C for 1 h. A schematic of the preparation of microcomposite filaments using a PDMS microfluidic channel is shown in Fig. 1.

Zeta Potential

The zeta potential of the CNC/AL spinning suspension (0.1 wt%) was determined using a zeta potential analyzer (Zetasizer Nano ZSP, Malvern Panalytical, Ltd., Worcestershire, UK) at the Central Laboratory of the Kangwon National University. The zeta potential of each sample was calculated using Henry's equation (Eq. 1), and the average value was obtained from three repeated measurements, as follows,

$$U_E = \frac{2\varepsilon\zeta}{3\eta} f(\kappa\alpha) \quad (1)$$

where U_E is the electrophoretic mobility ($\mu\text{m cm V}^{-1} \text{s}^{-1}$), ε is the dielectric constant, ζ is the zeta potential (mV), η is the viscosity (cP), and $f(\kappa\alpha)$ is Henry's function.

Morphological Characteristics

The morphological characteristics of the CNCs were observed by tapping mode using an atomic force microscope (AFM) (Nanoscope 5, Bruker, Billerica, USA) at the Central Laboratory of the Kangwon National University. CNC samples for AFM analysis were prepared as follows: Mica disks were immersed in 1% PEI solution for 10 min and air-dried for 30 min. Then, 0.05 wt% CNC suspension was dropped on the mica disk and spin-coated using a spin coater (ACE-200, Dong-ah Trade Corp., Seoul, Republic of Korea) at 3,000 rpm for 1 min. See details of morphological characteristics observed using AFM in Supporting Information (Fig. S1).

The morphological characteristics of wet-spun microcomposite filaments were observed using a scanning electron microscope (SEM; S-4800, Hitachi, Ltd., Tokyo, Japan) at the Central Laboratory of the Kangwon National University. The wet-spun microcomposite filaments were placed on aluminum stubs and iridium-coated to a thickness of 2 nm using a sputter coater (EMACE600, Leica Microsystems, Ltd., Wetzlar, Germany), which were then observed by SEM analysis at an accelerating voltage of 1 kV and working distance of 8.5 mm.

2D X-ray Diffraction (2D-XRD)

To analyze the orientation degree of CNC in the wet-spun microcomposite filaments, 2D-XRD analysis was carried out using a 2D-XRD analyzer (Bruker D8 Discover with Vantec 500 detector, Bruker Corp., Karlsruhe, Germany) with Cu-K α radiation ($\lambda = 1.5406 \text{ \AA}$) at the Korea Basic Science Institute, Daegu Center. The 2D-XRD patterns were recorded with an accelerating voltage of 40 kV, accelerating current of 40 mA, and beam size of 1.0 mm. A total of 40 microcomposite filaments were bundled

together to obtain sufficient intensity. From the 2D-XRD diffractogram, the orientation index (α) of CNC in the microcomposite filaments was calculated using Eq. 2 by azimuthal breadth analysis,

$$\text{Orientation index } (\alpha) = (180 - \beta_c)/180 \quad (2)$$

where β_c is the half-width of the azimuthal direction of the equatorial reflection of the (200) plane obtained from the 2D XRD patterns.

Tensile Properties

The wet-spun microcomposite filaments were kept in a thermo-hygrostat at a relative humidity of 30% to minimize the influence of variation in relative humidity on the tensile strength. The mechanical properties were measured (ASTM D3822-07) with a universal testing machine by applying a load cell of 0.5 N, gauge length of 10 mm, and cross-head speed of 3 mm/min. Five specimens of each sample were tested, and the average values of tensile strength, elastic modulus, and elongation at break were reported.

RESULTS AND DISCUSSION

Zeta Potential of CNC/AL Spinning Suspension

Table 1 shows the zeta potential values of the CNC, AL, and CNC/AL (95/5) mixtures. The values of all samples ranged from -47.8 to -73.3 mV, showing that the surface of all samples was strongly negatively charged. These negative surface charges of CNC and AL are due to ester sulfate groups on CNCs imparted during sulfuric acid hydrolysis and the carboxyl groups of AL, respectively (Siqueira *et al.* 2019). The zeta potential of -73.3 mV of CNC/AL (95/5) mixture is expected to have enhanced stable colloidal properties and improve their coagulation and gelation in the coagulation bath.

Table 1. Zeta Potential of CNC, AL, and CNC/AL (95/5) Spinning Suspension at a Concentration of 0.1 wt%

Sample	pH	Zeta potential (mV)
CNC	6.5	-47.8 ± 0.5
AL	7.0	-68.5 ± 3.3
CNC/AL (95/5)	6.7	-73.3 ± 2.1

Wet-spinnability of CNC

Figure 2 shows the effect of the type of coagulation solvent on the wet-spinnability of the CNC suspension. Isopropyl alcohol, 1,4-dioxane, sodium polyacrylate, and 10% CaCl₂ solution were used as coagulation solvents. The wet-spinning of CNC was more suitable in CaCl₂ solution than in isopropyl alcohol, 1,4-dioxane, and sodium polyacrylate. The negatively charged carboxylate (COO⁻) group or sulfate ester (SOO⁻) can generate crosslinking with positively charged ions, such as divalent calcium cations (Ca²⁺) (Grabowska *et al.* 2015; Liu and Li 2016). Because CNC has a sulfate group with a sulfur content of 0.94%, partial coagulation of the CNC in the CaCl₂ solution might improve the wet-spinnability.

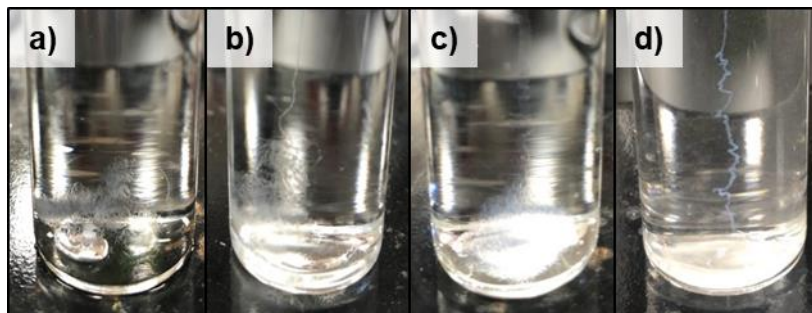


Fig. 2. Effect of the type of coagulation solvent on the wet-spinnability from 11.5 wt% of CNC suspension; a) Isopropyl alcohol, b) 1,4-dioxane, c) sodium polyacrylate, and d) CaCl_2

Figure 3 shows the appearance and coagulation of wet-spun microfilaments of CNC suspensions with different concentrations in CaCl_2 solution. With an increasing concentration of CNC, the spinnability improved. At concentrations lower than 6 wt%, the microfilament shape could not be obtained. At an 11.5 wt% concentration, a good shape of microfilaments was obtained. At a concentration above 11.5 wt%, the viscosity of CNC was too high to apply the microfluidic channel; thus, the concentration of 11.5 wt% was established as a maximum concentration for wet-spinning in the microfluidic channel.

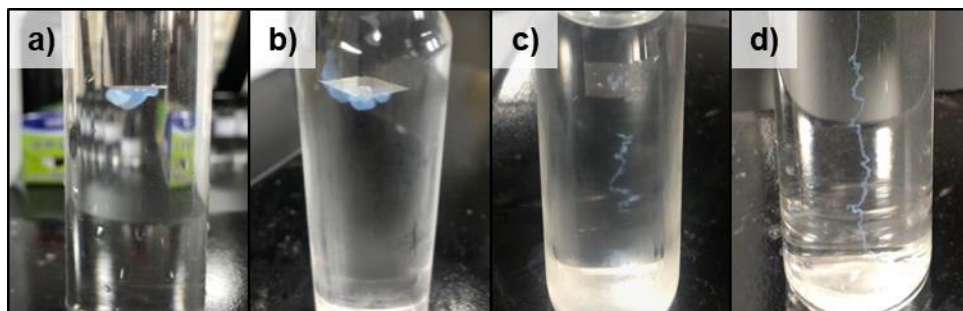


Fig. 3. Appearance of wet-spun microfilaments of CNC suspension without AL in CaCl_2 solution. Notes: CNC concentrations; a) 3.5 wt%, b) 6.0 wt%, c) 8.5 wt%, and d) 11.5 wt%

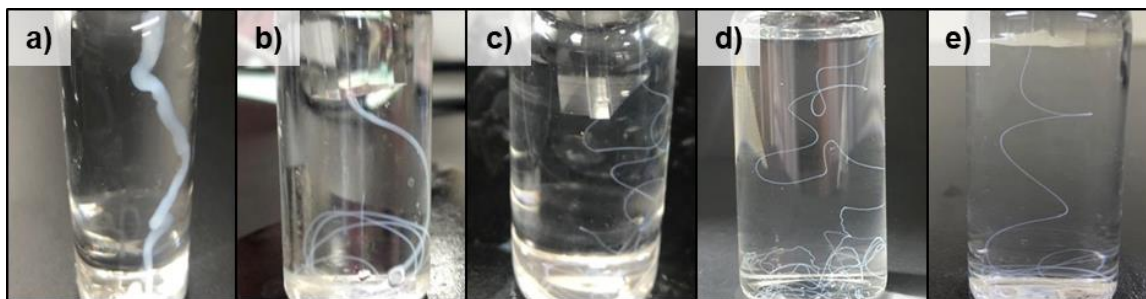


Fig. 4. Appearance of wet-spun microcomposite filaments from CNC/AL spinning suspension with different ratios of CNC/AL in CaCl_2 solution. The concentration and ratio of CNC/AL spinning suspension; a) 8.5 wt%, 99/1, b) 8.5 wt%, 97/3, c) 8.5 wt%, 95/5, d) 8.5 wt%, 90/10, and e) 11.5 wt%, 90/10

To improve the wet-spinnability and coagulation of CNC into microfilaments, AL was added to the CNC suspensions as a binder. Figure 4 shows the appearance of wet-spun microcomposite filaments of CNC/AL suspensions with different ratios of CNC/AL in CaCl_2 solution at concentrations of 8.5 and 11.5 wt%. With increasing AL content in CNC

suspension, wet-spinnability was radically improved, showing the best shape of the microcomposite filament at 10 wt% of AL addition. This phenomenon occurred due to the well-known Ca^{2+} ions induced gelling behavior of AL (Zheng *et al.* 2019). The gelled AL can act as a binder between the CNCs, which can result in the improvement of the wet-spinnability. The effect of AL content on the wet-spinnability of microcomposite filaments from the CNC/AL spinning suspension is shown in Table 2.

Table 2. Effect of AL Content on the Wet-Spinnability of Microcomposite Filaments from CNC/AL Spinning Suspension with Different Ratios of CNC/AL

Sample	Concentration (wt%)	Wet-spinnability *
CNC	3.5	+
CNC	6.0	+
CNC	8.5	++
CNC	11.5	+++
CNC/AL (99/1)	8.5	+++
CNC/AL (97/3)	8.5	++++
CNC/AL (95/5)	8.5	++++
CNC/AL (90/10)	8.5	++++
CNC/AL (90/10)	11.5	++++

Notes: spinning rate of CNC and CNC/AL, 10 $\mu\text{L}/\text{min}$; *wet-spinnability; spinning is impossible (+), spinning is possible but formed of short microcomposite filaments (++) , spinning is possible and formed of long microcomposite filaments (+++), spinning is possible and formed of long microcomposite filaments, and the microcomposite filaments are easily obtained from the collecting solvent (++++).

Morphological Characteristics of CNC/AL Microcomposite Filaments

Figure 5 shows the morphological characteristics of wet-spun microcomposite filaments made with CNC/AL spinning suspension at different ratios of CNC/AL, concentration of suspension, and spinning rate. All the microcomposite filaments showed linear fibrous structures. With increasing AL content in CNC suspension at the same spinning rate, the diameter tended to decrease, but the surface morphology became coarse. The decrease in the diameter might be due to the great compatibility and attractive forces between the two hydrophilic biopolymers and similar behavior was also observed with CNF in our previous study (Park *et al.* 2021). Because of this decrease in diameter, the rod-like CNC structures will appear prominently and make the coarse surface. However, as the pure AL is known to form smooth fibers, it is assumed that this behavior will be observed only when low content of AL is used. Furthermore, as the spinning rate and spinning suspension concentration increased in CNC/AL (95/5), the surface became rougher, showing some cracks on the surface. The average diameters of wet-spun microcomposite filaments under different spinning conditions are summarized in Table 3. As the AL content increased from 3% and 5% to 10% in the CNC/AL spinning suspension, the average diameter decreased from 114.7, 82.2, and 72.6 μm , respectively. In CNC/AL (95/5) microcomposite filaments, the average diameter decreased as the concentration and spinning rate increased.

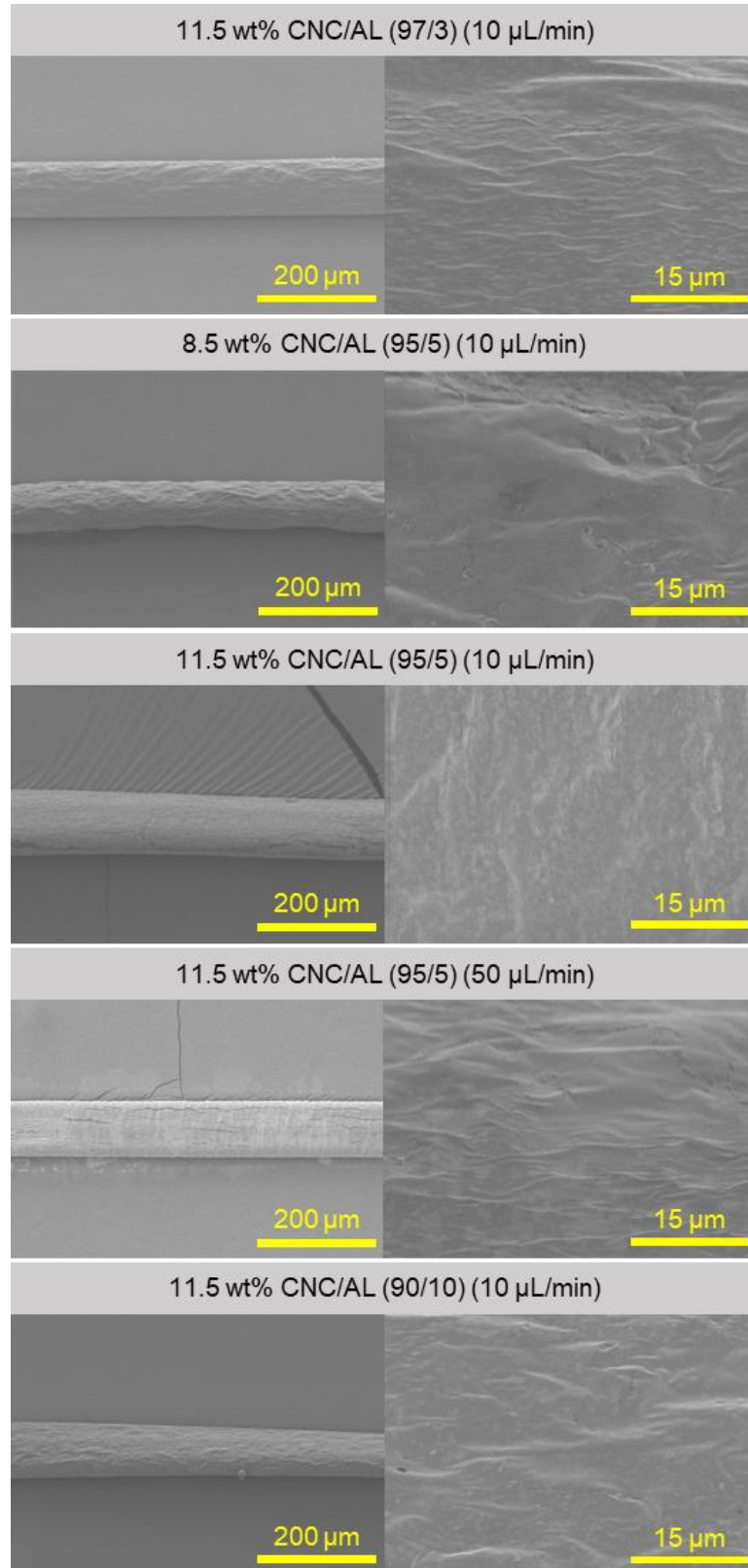


Fig. 5. Effect of AL content, concentration, and spinning rate on the morphological characteristics of wet-spun microcomposite filaments formed of CNC/AL spinning suspension

Table 3. Average Diameters and Orientation Indexes of Wet-Spun Microcomposite Filaments Formed of CNC/AL Spinning Suspension

Sample	Ratio of CNC/AL	Concentration (wt%)	Spinning Rate ($\mu\text{L}/\text{min}$)	Average Diameter (μm)	Orientation index
CNC/AL	97/3	11.5	10	114.7 ± 9.1	0.439
CNC/AL	95/5	8.5	10	88.9 ± 3.0	0.494
		11.5	10	82.2 ± 6.8	0.498
			50	74.8 ± 3.0	0.506
CNC/AL	90/10	11.5	10	72.6 ± 1.9	0.366

Orientation Index

Figure 6 shows the 2D X-ray diffractogram of the wet-spun microcomposite filament formed of CNC/AL spinning suspension under different AL content, concentration, and spinning rate. Randomly oriented CNCs show ring patterns, and CNC oriented in one direction produces arc patterns in 2D X-ray diffractograms (Ahvenainen *et al.* 2016; Park *et al.* 2020). In the microcomposite filaments formed of CNC/AL, strong reflections with two arc patterns were observed at the middle azimuth. This is because the CNCs are aligned in the wet-spun microcomposite filament along the axis of the filament. The orientation index was calculated from the azimuthal profiles of the (200) reflections and shown inside the 2D X-ray diffractogram. The orientation index of the wet-spun microcomposite filament formed of CNC/AL spinning suspension under different spinning conditions are summarized in Table 3.

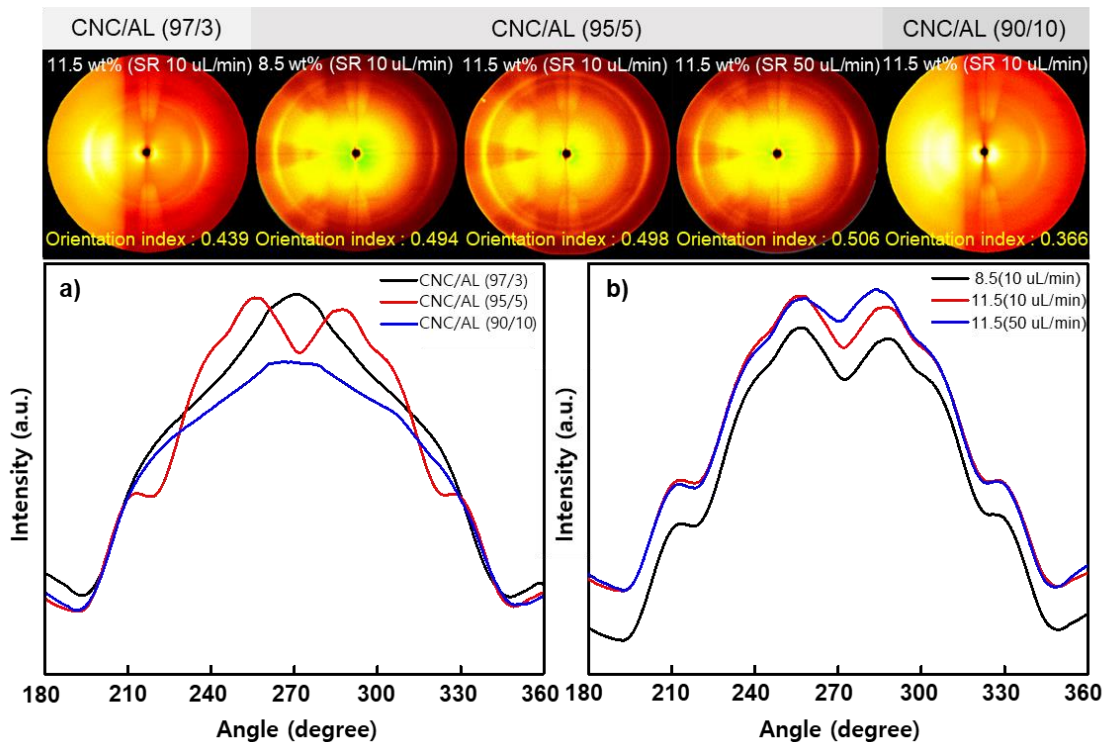


Fig. 6. Azimuthal profiles of the (200) reflections from the 2D X-ray diffractogram of the wet-spun microcomposite filaments; a) microcomposite filaments formed of 11.5 wt% CNC/AL spinning suspensions with different AL content, b) formed of CNC/AL (95/5) spinning suspension with different concentrations and spinning rates

In CNC/AL (95/5) microcomposite filaments, the microcomposite filaments indicated similar values of the orientation index of 0.494 to 0.506. As the spinning rate increased from 10 to 50 $\mu\text{L}/\text{min}$, it increased slightly from 0.498 to 0.506. Iwamoto *et al.* (2011) prepared TOCNF from wood and tunicate and successfully manufactured filaments through the wet-spinning process using a microneedle in acetone. They reported that the orientation index was 0.65 to 0.72, which increased with an increasing spinning rate from 0.1 to 100 mL/min . As the AL content increased to 10% in the CNC/AL spinning suspension, however, the orientation index decreased to 0.366. An increase in the amorphous AL content disturbed the alignment of CNCs in the wet-spun microcomposite filament.

Tensile Properties

Table 4 shows the tensile strength, elastic modulus, and elongation at break of the wet-spun microcomposite filaments formed from CNC/AL spinning suspension with different ratios of CNC/AL, concentration, and spinning rates. As the AL content increased in the spinning suspension, the tensile strength and elastic modulus of the wet-spun microcomposite filaments tended to decrease. This is because AL has lower mechanical properties because of its amorphous phase compared to CNC. Similar result was observed in a previous study by Phisalaphong *et al.* (2008). The authors prepared a BNC/AL membrane by coagulating a BNC/AL in a 5% aqueous calcium chloride solution followed by a 1% HCl solution. As the AL content increased from 20% to 80%, the tensile strength of the BNC/AL composite membrane decreased from 3.38 to 1.67 MPa. There was no significant difference between the tensile strength of the microcomposite filament wet-spun at 8.5 wt% and that spun at 11.5 wt%. In samples formed of 11.5 wt% CNC/AL (95/5), as the spinning rate increased from 10 to 50 $\mu\text{L}/\text{min}$, the tensile strength and elastic modulus tended to improve. The increased orientation index of CNC can improve the tensile properties of microcomposite filaments (Park *et al.* 2020; Iwamoto *et al.* 2011). Kafy *et al.* (2017) prepared TOCNF filaments *via* wet-spinning and investigated the effect of spinning rate on the orientation index and mechanical properties of wet-spun filaments. They found that an increase in the spinning rate caused an increase in the TOCNF orientation index, which resulted in an improvement in the tensile properties.

Table 4. Tensile Strength, Elastic Modulus, and Elongation at Break of the Wet-Spun Microcomposite Filaments Formed of CNC/AL Spinning Suspension with Different AL Content, Concentration, and Spinning Rates

Sample	Concentration (wt%)	Spinning Rate ($\mu\text{L}/\text{min}$)	Tensile Strength (MPa)	Elastic Modulus (MPa)	Elongation at Break (%)
CNC/AL (97/3)	11.5	10	10.5 \pm 1.0	1040.5 \pm 88.0	2.9 \pm 0.7
CNC/AL (95/5)	8.5	10	11.9 \pm 0.1	769.8 \pm 47.6	6.3 \pm 1.3
	11.5	10	11.7 \pm 3.7	936.5 \pm 189.6	9.3 \pm 0.9
		50	17.5 \pm 1.2	1750.3 \pm 86.7	6.6 \pm 0.7
CNC/AL (90/10)	11.5	10	6.2 \pm 1.4	317.4 \pm 71.2	3.3 \pm 0.8

CONCLUSIONS

1. Wet-spinning of cellulose nanocrystal (CNC) suspensions was successfully performed using a microfluidic channel, and microfilaments were fabricated.
2. Isopropyl alcohol, 1,4-dioxane, sodium polyacrylate, and CaCl₂ solution were tested as prospective coagulation solvents, and CaCl₂ solution was found as the appropriate solvent for the formation of the filament.
3. Sodium alginate (AL) was used as filler, and the effect of wet-spinning conditions including AL content on the wet-spinnability and filament properties was investigated. The addition of AL resulted in improved wet-spinnability of the CNC suspension due to the gelation of AL by ion bonds with Ca²⁺.
4. As the AL content increased from 3% and 5% to 10%, the average diameter decreased from 114.7, 82.2, and 72.6 μm.
5. In CNC/AL (95/5) microcomposite filaments, as the spinning rate increased from 10 to 50 μL/min, due to the improved orientation index the tensile strength and elastic modulus were improved from 11.7 to 17.5 MPa and 936.5 to 1750.3 MPa, respectively.

ACKNOWLEDGMENTS

This research was supported by the National Institute of Forest Science (FP0400-2016-01) grant, 'R&D Program for Forest Science Technology (2019151D10-2123-0301)' provided by Korea Forest Service (Korea Forestry Promotion Institute), and by the Basic Science Research Program through the National Research Foundation of Korea (NRF) funded by the Ministry of Education (No. 2018R1A6A1A03025582).

REFERENCES CITED

- Abitbol, T., Rivkin, A., Cao, Y., Nevo, Y., Abraham, E., Ben-Shalom, T., Lapidot, S., and Shoseyov, O. (2016). "Nanocellulose, a tiny fiber with huge applications," *Current Opinion in Biotechnology* 39, 76-88. DOI: 10.1016/j.copbio.2016.01.002
- Ahvenainen, P., Kontro, I., and Svedström, K. (2016). "Comparison of sample crystallinity determination methods by X-ray diffraction for challenging cellulose I materials," *Cellulose* 23(2), 1073-1086. DOI: 10.1007/s10570-016-0881-6
- Ávila, H. M., Schwarz, S., Rotter, N., and Gatenholm, P. (2016). "3D bioprinting of human chondrocyte-laden nanocellulose hydrogels for patient-specific auricular cartilage regeneration," *Bioprinting* 1, 22-35. DOI: 10.1016/j.bprint.2016.08.003
- Bonhomme, O., Leng, J., and Colin, A. (2012). "Microfluidic wet-spinning of alginate microfibers: A theoretical analysis of fiber formation," *Soft Matter* 8, 10641-10649. DOI: 10.1039/C2SM25552A
- Cheng, M., Qin, Z., Chen, Y., Hu, S., Ren, Z., and Zhu, M. (2017). "Efficient extraction of cellulose nanocrystals through hydrochloric acid hydrolysis catalyzed by inorganic chlorides under hydrothermal conditions," *ACS Sustainable Chem. Eng.* 5(6), 4656-4664. DOI: 10.1021/acssuschemeng.6b03194

- Grabowska, B., Sitarz, M., Olejnik, E., Kaczmarska, K., and Tyliszczak, B. (2015). "FT-IR and FT-Raman studies of cross-linking processes with Ca²⁺ ions, glutaraldehyde and microwave radiation for polymer composition of poly (acrylic acid)/sodium salt of carboxymethyl starch–In moulding sands, Part II," *Spectrochimica Acta Part A: Molecular and Biomolecular Spectroscopy* 151, 27-33. DOI: 10.1016/j.saa.2015.06.084
- Gursoy, A., Iranshahi, K., Wei, K., Tello, A., Armagan, E., Boesel, L. F., Sorin, F., Rossi, R. M., Defraeye, T., and Toncelli, C. (2020). "Facile fabrication of microfluidic chips for 3D hydrodynamic focusing and wet spinning of polymeric fibers," *Polymers* 12(3), 633. DOI: 10.3390/polym12030633
- Habibi, Y., Lucia, L. A., and Rojas, O. J. (2010). "Cellulose nanocrystals: Chemistry, self-assembly, and applications," *Chemical Reviews* 110(6), 3479-3500. DOI: 10.1021/cr900339w
- Haynl, C., Hofmann, E., Pawar, K. Förster, S., and Scheibel, T. (2016). "Microfluidics-produced collagen fibers show extraordinary mechanical properties," *Nano Letters* 16(9), 5917-5922. DOI: 10.1021/acs.nanolett.6b02828
- Hubbe, M. A., Ferrer, A., Tyagi, P., Yin, Y., Salas, C., Pal, L., and Rojas, O. J. (2017). "Nanocellulose in thin films, coatings, and plies for packaging applications: A review," *BioResources* 12(1), 2143-2233.
- Iwamoto, S., Isogai, A., and Iwata, T. (2011). "Structure and mechanical properties of wet-spun fibers made from natural cellulose nanofibers," *Biomacromolecules* 12(3), 831-836. DOI: 10.1021/bm101510r
- Jun, Y., Kang, E., Chae, S., and Lee, S. H. (2014). "Microfluidic spinning of micro- and nano- scale fibers for tissue engineering," *Lab on a Chip* 14, 2145-2160. DOI: 10.1039/C3LC51414E
- Kafy, A., Kim, H. C., Zhai, L., Kim, J. W., Hai, L. V., and Kang, T. J. (2017). "Cellulose long fibers fabricated from cellulose nanofibers and its strong and tough characteristics," *Scientific Reports* 7(1), 1-8. DOI: 10.1038/s41598-017-17713-3
- Khalil, H. A., Bhat, A. H., Bakar, A. A., Tahir, P. M., Zaidul, I. S. M., and Jawaid, M. (2015). "Cellulosic nanocomposites from natural fibers for medical applications: A review," *Handbook of polymer nanocomposites. Processing, performance and application*, 475-511. DOI: 10.1007/978-3-642-45232-1_72
- Köse, K., Mavlan, M., and Youngblood, J. P. (2020). "Applications and impact of nanocellulose based adsorbents," *Cellulose* 27(6), 2967-2990. DOI: 10.1007/s10570-020-03011-1
- Lee, B. R., Lee, K. H., Kang, E., Kim, D. S., and Lee, S. H. (2011). "Microfluidic wet spinning of chitosan-alginate microfibers and encapsulation of HepG2 cells in fibers," *Biomicrofluidics* 5(2), 22208. DOI: 10.1063/1.3576903
- Lee, S. H., Kim, H. J., and Kim, J. C. (2019). "Nanocellulose applications for drug delivery: A review," *Journal of Forest and Environmental Science* 35(3), 141-149. DOI: 10.7747/JFES.2019.35.3.141
- Lennartsson, P. R., Niklasson, C., and Taherzadeh, M. J. (2011). "A pilot study on lignocelluloses to ethanol and fish feed using NMMO pretreatment and cultivation with zygomycetes in an air-lift reactor," *Bioresource Technology* 102(6), 4425-4432. DOI: 10.1016/j.biortech.2010.12.089
- Liu, J., Zhang, R., Ci, M., Sui, S., and Zhu, P. (2019). "Sodium alginate/cellulose nanocrystal fibers with enhanced mechanical strength prepared by wet spinning," *Journal of Engineered Fibers and Fabrics* 14, 1-7. DOI: 10.1177/1558925019847553

- Liu, S., and Li, L. (2016). "Thermoreversible gelation and scaling behavior of Ca²⁺-induced κ -carrageenan hydrogels," *Food Hydrocolloids* 61, 793-800. DOI: 10.1016/j.foodhyd.2016.07.003
- Lundahl, M. J., Cunha, A. G., Rojo, E., Papageorgiou, A. C., Rautkari, L., Arboleda, J. C., and Rojas, O. J. (2016a). "Strength and water interactions of cellulose I filaments wet-spun from cellulose nanofibril hydrogels," *Scientific reports* 6(1), 1-13. DOI: 10.1038/srep30695
- Lundahl, M. J., Klar, V., Wang, L., Ago, M., and Rojas, O. J. (2016b). "Spinning of cellulose nanofibrils into filaments: A review," *Industrial & Engineering Chemistry Research* 56(1), 8-19. DOI: 10.1021/acs.iecr.6b04010
- Nechyporchuk, O., and Köhnke, T. (2018). "Regenerated casein–nanocellulose composite fibers via wet spinning," *ACS Sustainable Chemistry & Engineering* 7(1), 1419-1426. DOI: 10.1021/acssuschemeng.8b05136
- Park, C. W., Park, J. S., Han, S. Y., Lee, E. A., Kwon, G. J., Seo, Y. H., Gwon, J. G., Lee, S. Y., and Lee, S. H. (2020). "Preparation and characteristics of wet-spun filament made of cellulose nanofibrils with different chemical compositions," *Polymers* 12(4), 949. DOI: 10.3390/polym12040949
- Park, J. S., Park, C. W., Han, S. Y., Lee, E. A., Cindradewi, A. W., Kim, J. K., Kwon, G. J., Seo, Y. H., Yoo, W. J., Gwon, J., and Lee, S. H. (2021). "Preparation and properties of wet-spun microcomposite filaments from various CNFs and alginate," *Polymers* 13(11), 1709. DOI: 10.3390/polym13111709
- Phisalaphong, M., Suwanmajo, T., and Tammarate, P. (2008). "Synthesis and characterization of bacterial cellulose/alginate blend membranes," *Journal of Applied Polymer Science* 107(5), 3419-3424. DOI: 10.1002/app.27411
- Plecis, A., and Chen, Y. (2007). "Fabrication of microfluidic devices based on glass-PDMS-glass technology," *Microelectronic Engineering* 84(5-8), 1265-1269. DOI: 10.1016/j.mee.2007.01.276
- Sayyed, A. J., Deshmukh, N. A., and Pinjari, D. V. (2019). "A critical review of manufacturing processes used in regenerated cellulosic fibres: Viscose, cellulose acetate, cuprammonium, LiCl/DMAc, ionic liquids, and NMMO based lyocell," *Cellulose* 26(5), 2913-2940. DOI: 10.1007/s10570-019-02318-y
- Sen, S., Patil, S., and Argyropoulos, D. S. (2015). "Thermal properties of lignin in copolymers, blends, and composites: A review," *Green Chemistry* 17(11), 4862-4887. DOI: 10.1039/C5GC01066G
- Shang, L., Yu, Y., Liu, Y., Chen, Z., Kong, T., and Zhao, Y. (2019). "Spinning and applications of bioinspired fiber systems," *ACS nano* 13(3), 2749-2772. DOI: 10.1021/acsnano.8b09651
- Siqueira, P., Siqueira, É., De Lima, A. E., Siqueira, G., Pinzón-García, A. D., Lopes, A. P., Segura, M. E. C., Isaac, A., Pereira, F. V., and Botaro, V. R. (2019). "Three-dimensional stable alginate-nanocellulose gels for biomedical applications: Towards tunable mechanical properties and cell growing," *Nanomaterials* 9(1), 78. DOI: 10.3390/nano9010078
- Syverud, K., Pettersen, S. R., Draget, K., and Chinga-Carrasco, G. (2015). "Controlling the elastic modulus of cellulose nanofibril hydrogels-scaffolds with potential in tissue engineering," *Cellulose* 22(1), 473-481. DOI: 10.1007/s10570-014-0470-5
- Tan, T. H., Lee, H. V., Dabdawb, W. A. Y., and Abd Hamid, S. B. B. O. (2019). "A review of nanocellulose in the drug-delivery system," *Materials for Biomedical Engineering*, 131-164. DOI: 10.1016/B978-0-12-816913-1.00005-2

- Whitesides, G. M. (2006). "The origins and the future of microfluidics," *Nature* 442, 368-373. DOI: 10.1038/nature05058
- Xia, Y., and Whitesides, G. M. (1998). "Soft lithography," *Annual Review of Materials Science* 28, 153-184. DOI: 10.1146/annurev.matsci.28.1.153
- Xu, G. K., Liu, L., and Yao, J. M. (2013). "Fabrication and characterization of alginate fibers by wet-spinning," *Advanced Materials Research* 796, 87-91. DOI: 10.4028/www.scientific.net/AMR.796.87
- Zhang, S., and Luo, J. (2011). "Preparation and properties of bacterial cellulose/alginate blend bio-fibers," *Journal of Engineered Fibers and Fabrics* 6(3), 69-72. DOI: 10.1177/155892501100600309
- Zheng, J., Zeng, R., Zhang, F., and Kan, J. (2019). "Effects of sodium carboxymethyl cellulose on rheological properties and gelation behaviors of sodium alginate induced by calcium ions," *LWT - Food Science and Technology* 103, 131-138. DOI: 10.1016/j.lwt.2018.12.081

Article submitted: April 19, 2021; Peer review completed: June 1, 2021; Revised version received and accepted: June 28, 2021; Published: July 2, 2021.
DOI: 10.15376/biores.16.3.5780-5793